α-cluster states in intermediate mass nuclei

Peter Mohr*
Diakonie-Klinikum Schwäbisch Hall, D-74523 Schwäbisch Hall, Germany
(Dated: March 14, 2008)

Properties of intermediate mass nuclei have been investigated within the framework of the α-cluster model in combination with systematic double-folding potentials. Previously, this α-cluster model has been widely applied to light nuclei, in particular to ^{8}Be = $\alpha \otimes \alpha$, ^{20}Ne = ^{16}O $\otimes \alpha$, and ^{44}Ti = ^{40}Ca $\otimes \alpha$, and to heavy nuclei, in particular to ^{212}Po = ^{208}Pb $\otimes \alpha$. In the present work a wide range of nuclei is investigated with the magic neutron number $N = 50$ in the mass range around $A \approx 80 - 100$: (A+4,N=52) = (A,N=50) $\otimes \alpha$. It is found that excitation energies, decay properties, and transition strengths can be described successfully within this model. The smooth and small variation of the underlying parameters of the α-nucleus potential may be used for extrapolations to predict experimentally unknown properties in the nuclei under study.

PACS numbers: 21.60.Gx,27.50.+e,27.60.+j

I. INTRODUCTION

Atomic nuclei are complex many-body systems. Their properties are defined by the short-range nuclear interaction and the long-range Coulomb interaction which have to be included in the quantum-mechanical many-body Schroedinger equation. The many-body problem may be dramatically simplified in some cases where the nucleus can be considered to be composed of two inert clusters like an α-particle and a closed-shell nucleus. In these cases a simple two-body model is able to reproduce many properties like e.g. excitation energies and decay properties – provided that the interaction potential can be well described. This α-cluster model has been widely applied to light nuclei, in particular to ^{8}Be = $\alpha \otimes \alpha$, ^{20}Ne = ^{16}O $\otimes \alpha$, and ^{44}Ti = ^{40}Ca $\otimes \alpha$, and to heavy nuclei, in particular to ^{212}Po = ^{208}Pb $\otimes \alpha$. Here I apply this α-cluster model in combination with systematic α-nucleus double-folding potentials to the analysis of a wide range of nuclei with the magic neutron number $N = 50$ in the mass range around $A \approx 80 - 100$: (A+4,N=52) = (A,N=50) $\otimes \alpha$. This study extends earlier work which has focused on ^{94}Mo = ^{90}Zr $\otimes \alpha$.

The α-particle is the lightest doubly-magic nucleus. Thus it is strongly bound, and its first excited state is located at the high excitation energy $E_x = 20.2\,\mathrm{MeV}$ [1, 2]. Although composed of four nucleons, the α-particle may be considered as inert in many investigations, i.e. the internal structure of the α-particle may be neglected. It has been stated that this "concept of α-clustering is essential for understanding the structure of light nuclei" [3], and this concept has been extended to heavy nuclei (e.g. [4, 5, 6, 7, 8, 9, 10]).

As a consequence of the strong binding of α-particles many observables in the interaction of two α-particles can be described successfully using a simple two-body model. Typical observables are scattering cross sections of the ^{4}He(α,α)^{4}He reaction and excitation energies, transition probabilities, and decay properties of the ^{8}Be = $\alpha \otimes \alpha$ nucleus. A prerequisite for the successful application of the simple two-body model is an effective potential between the two α-particles. It has been shown that the double-folding potential and the widely used DDM3Y interaction provide an excellent description of the above observables [11].

Similar arguments hold for the description of nuclei which are composed of another doubly-magic nucleus and an α-particle, and numerous studies have been devoted to ^{20}Ne = ^{16}O $\otimes \alpha$, ^{44}Ti = ^{40}Ca $\otimes \alpha$, and ^{212}Po = ^{208}Pb $\otimes \alpha$ (see e.g. the review papers of the dedicated special issue of Prog. Theor. Phys. Suppl. **132**, [3, 4, 5, 6, 7, 8, 9, 10]). However, there is no stable doubly-magic nucleus with the magic neutron number $N = 50$. In the present work I analyze nuclei with (A+4,N=52) = (A,N=50) $\otimes \alpha$ between the two instable $N = 50$ doubly-magic nuclei ^{78}Ni ($Z = 28$) and ^{100}Sn ($Z = 50$). Previous studies (e.g. [4, 12, 13]) have been restricted to ^{94}Mo = ^{90}Zr $\otimes \alpha$ because of the subshell closure at $Z = 40$ between f and p subshells and the proton $g_{9/2}$ subshell. It will be shown that there is no need for this restriction. The proton subshell closure at $Z = 40$ turns out to be not important for the properties of α-cluster states. Instead, the α-cluster model can be applied successfully in the same way to all nuclei under study except the semi-magic $Z = 50$ nucleus ^{102}Sn = ^{98}Cd $\otimes \alpha$. The present study is restricted to even-even nuclei. An extension of the present study to even-odd nuclei is possible e.g. for ^{93}Nb = ^{89}Y $\otimes \alpha$ which will be published together with the analysis of the ^{89}Y(α,α)^{89}Y scattering cross section [14].

The paper is organized as follows. In Sect. II the ingredients of the simple two-body model are briefly summarized. In particular, the underlying double-folding potential and the formalism for the calculation of bound state properties and transition strengths is presented. In Sect. III the results of the calculations, i.e. the systematic behavior of the potential parameters for the description of the bound state energies, are shown. Sect. IV gives a discussion of the results, and finally conclusions

*Electronic address: WidmaierMohr@compuserve.de

are drawn in Sect. V. In the following discussion proton (neutron, mass) numbers N_C (Z_C, A_C) of the compound nucleus (A_C=A+4,N_C=N+2) = (A,N) $\otimes$ α are indexed by the subscript C whereas Z (N, A) without index refers to the core nucleus; e.g., properties of the $N_C = 52$, $Z_C = 42$, $A_C = 94$ nucleus ^{94}Mo are calculated from the potential between the $N = 50$, $Z = 40$, $A = 90$ core ^{90}Zr $\otimes$ α.

II. INGREDIENTS OF THE MODEL

A. Folding potentials

The basic ingredient of the present study is the α-nucleus potential. Various parametrizations have been used in literature. However, recent systematic studies have concentrated on folding potentials and Woods-Saxon potentials. It has been shown that the parameters of folding potentials, in particular the volume integral J_R, show a very systematic behavior for intermediate and heavy mass nuclei [15]. This study [15] has been extended to the analysis of elastic scattering data at astrophysically relevant energies around the Coulomb barrier [16, 17, 18, 19, 20]. Experimental data for (α,γ) capture reactions and other α-induced reactions like (α,n) have been studied using folding potentials and other potential parametrizations, see e.g. in [21, 22, 23, 24]. Further information on the systematics of folding potentials has been obtained from the analysis of α-decay data for superheavy nuclei (e.g. [25, 26, 27, 28, 29, 30, 31]), for neutron-deficient p-nuclei [32, 33, 34], and for nuclei slightly above the doubly-magic $N = Z = 50$ nucleus ^{100}Sn [35, 36]. The present work extends the study of [36] to lighter $N = 50$ nuclei because the double-folding potentials have proven to be reliable in such a broad range of masses.

Global and local Woods-Saxon potentials have also been determined succssfully for the mass range under study in [37, 38, 39]. The description of scattering data is similar to folding potentials [20]. However, as will be shown in Sect. II B, it is not possible to obtain a reasonable description of the excitation energies of rotational bands in (A+4,N=52) = (A,N=50) $\otimes$ α nuclei.

Other parametrizations of the α-nucleus potential like e.g. modified Woods-Saxon potentials [13] or the so-called *cosh* potential [40] are not analyzed in this work. Although the *cosh* potential was able to describe α-decay properties, the *cosh* potential or other potentials have not been used for the simultaneous description of scattering and reaction cross sections and bound state and decay properties.

The double-folding potential $V_F(r)$ is calculated from the densities of the interacting nuclei and an effective nucleon-nucleon interaction. In the present work the nuclear densities were derived from electron scattering data which are compiled in [41]. Many nuclei under study are unstable, and electron scattering data are not available in [41]. Therefore, the densities for all $N = 50$ nuclei in the present study were derived in the same way as in [25, 36]; there it was shown that an averaged two-parameter Fermi distribution provides reasonable densities over a broad mass range by a simple scaling of the radius parameter $r \sim A^{1/3}$. As will be discussed later, the resuls do not show a strong dependence on the radius parameter. The widely used DDM3Y interaction is also applied in this work. Details on the calculation of the double-folding potential and the effective interaction can be found in [15, 42, 43, 44].

The total potential $V(r)$ is given by the sum of the nuclear potential $V_N(r)$ and the Coulomb potential $V_C(r)$:

$$V(r) = V_N(r) + V_C(r) = \lambda\, V_F(r) + V_C(r) \qquad (1)$$

The Coulomb potential is taken in the usual form of a homogeneously charged sphere where the Coulomb radius R_C has been chosen identically with the root-mean-square radius $r_{\rm rms}$ of the folding potential V_F. The folding potential V_F is scaled by a strength parameter λ which is of the order of $1.0 - 1.3$. This leads to volume integrals of about $J_R \approx 300\,\mathrm{MeV\,fm^3}$ for all nuclei under study and is in agreement with systematic α-nucleus potentials derived from elastic scattering [15, 21, 39]. (Note that as usual the negative sign of J_R is omitted in this work.)

For comparison, calculations have also been performed with nuclear potentials V_N of Woods-Saxon shape: $V_N(r) = V_0 \times [1 + \exp{(r - R)/a}]^{-1}$ with the potential depth V_0, radius parameter $R = r_0 \times A^{1/3}$ and diffuseness a.

It has been suggested that a temperature dependence of the optical potential may improve the simultaneous description of scattering, reaction, and decay data [38]. The analysis of scattering and reaction data requires a complex optical potential where the imaginary part describes the absorption into other channels. The present study focuses on bound state properties which can be calcuated from the real part of the potential, see Eq. (1). Because of the energy and density dependence of the interaction and because of the above mentioned temperature dependence it is clear that the real potentials from this study will require minor modification so that they can be used as real part of a complex potential in the analysis of scattering and reaction data.

B. Bound and quasi-bound states

From a given nuclear potential it is a straightforward task to calculate the eigenstates of the Hamilton operator, i.e. the energies E and wave functions $u(r)$. The Pauli principle is taken into account by the so-called Wildermuth condition which relates the quantum numbers Q, N, L of the α-particle to the quantum numbers q_i, n_i, l_i

of the four constituent nucleons:

$$Q = 2N + L = \sum_{i=1}^{4}(2n_i + l_i) = \sum_{i=1}^{4} q_i \qquad (2)$$

where Q is the number of oscillator quanta, N is the number of nodes and L the relative angular momentum of the α-core wave function, and $q_i = 2n_i + l_i$ are the corresponding quantum numbers of the four nucleons forming the α cluster. I have taken $q = 4$ for the two neutrons above the neutron number $N = 50$ and $q = 4$ ($q = 3$) for protons above (below) the proton number $Z = 40$. This leads to $Q = 16$ for nuclei above ^{94}Mo = ^{90}Zr $\otimes$ α and $Q = 14$ for nuclei below ^{92}Zr = ^{88}Sr $\otimes$ α.

In a first calculation the strength of the nuclear potential is adjusted to reproduce the binding energy E_B of the α-particle to the $N = 50$ core. E.g., for the 0^+ ground state wave function of the nucleus ^{96}Ru = ^{92}Mo $\otimes$ α one finds $E_B = -1692\,$keV [1] ($E_B < 0$ for bound states). For the folding potential a strength parameter of $\lambda = 1.1965$ is required to reproduce this energy with $Q = 16$, i.e., a wave function with angular momentum $L = 0$ and $N = 8$ nodes. For the Woods-Saxon potential one finds $V_0 = 142.97\,$MeV (162.38 MeV) using geometry parameters of $r_0 = 1.3\,$fm (1.2 fm) and $a = 0.7\,$fm. These geometry parameters of the Woods-Saxon potential are close to the Woods-Saxon potentials derived from scattering data [37, 38, 39]. The square of the wave functions $u(r)$ in the different potentials is shown in Fig. 1.

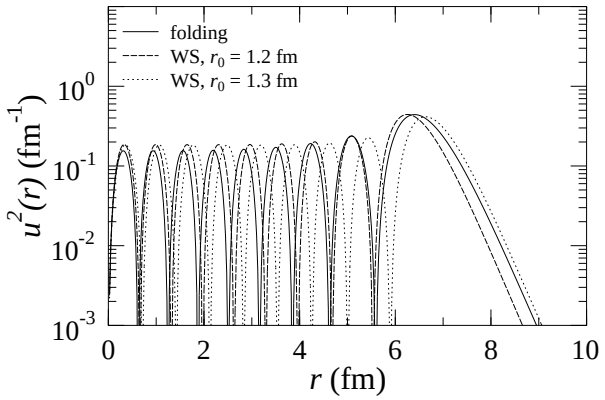

FIG. 1: Square of the wave function $u(r)$ of the 0^+ ground state of ^{96}Ru = ^{92}Mo $\otimes$ α at $E = -1692\,$keV using the folding potential with $\lambda = 1.1965$ and the Woods-Saxon potentials with two different radius parameters $r_0 = 1.2\,$fm and 1.3 fm. Corresponding to $Q = 16$, the number of nodes is eight.

In the next step the energies of all excited states with $Q = 16$ are calculated using exactly the same potential as for the ground state. The excitation energies E_x are defined by $E = E_B + E_x$. The result is shown in Fig. 2 for the chosen example of ^{96}Ru = ^{92}Mo $\otimes$ α. Experimentally states with quantum numbers from 0^+ to 16^+ are known which form a rotational band although the energies do not follow exactly the rigid rotator rule $\sim L(L+1)$. A similar rotational behavior is found for the folding potential; however, the excitation energies are much lower than the experimental values. In contrast, the Woods-Saxon potentials show an inversion of the levels; i.e., the 16^+ state is strongest bound in the Woods-Saxon potential. This finding is independent of details of the chosen geometry parameters. In Fig. 2 results for two radius parameters $r_0 = 1.2\,$fm and 1.3 fm are shown. Whereas in the case of the folding potential a minor readjustment of the potential strength of less than 5 % is sufficient to reproduce the excitation energies (see Sect. III), the Woods-Saxon potential requires strong modification of more than 20 % to reproduce the excitation energy spectrum.

It is interesting to note that the inversion of the excitation energies in the Woods-Saxon potential is not directly related to the width of the potential. As can be seen from Fig. 1, the wave function of the Woods-Saxon potential with $r_0 = 1.2\,$fm is concentrated at smaller radii than the folding wave function whereas the wave function in the Woods-Saxon potential with $r_0 = 1.3\,$fm is concentrated at larger radii. Nevertheless, both Woods-Saxon potentials show the inversion of excitation energies, whereas the folding potential reproduces a rotational band (see also Fig. 2).

C. Transition strengths

Reduced transition strengths $B(E\mathcal{L})$ for electromagnetic transitions $L_i \rightarrow L_f$ can be calculated from the bound state wave functions $u_{L_i}(r)$ and $u_{L_f}(r)$. The transition strengths scale with the square of the overlap integral

$$B(E\mathcal{L}) \sim \left| \int u_{L_f}(r)\, r^{\mathcal{L}}\, u_{L_i}(r)\, dr \right|^2 \qquad (3)$$

The full formalism for the calculation of $B(E\mathcal{L})$ values can be found e.g. in [45, 46, 47]. The present study will be restricted to quadrupole transitions with $\mathcal{L} = 2$. One expects enhanced transition strengths of the order of several Weisskopf units (W.u.) for the intraband transitions within a rotational band. The present study extends earlier work which has focused on transitions in ^{94}Mo = ^{90}Zr $\otimes$ α [4, 12, 13].

As an example, Fig. 3 shows the wave functions $u_{L=0}(r)$, $u_{L=2}(r)$, and the integrand of the overlap integral in Eq. (3) for the transition from the 2^+ state at $E_x = 833\,$keV to the 0^+ ground state in ^{96}Ru. The dominating contribution of the integral in Eq. (3) is located at the nuclear surface around $6 - 8\,$fm.

It is interesting to note that the calculated transition strengths $B(E\mathcal{L})$ show only a weak dependence on the excitation energy E_x wich is discussed now for the shown example of the $2^+ \rightarrow 0^+$ transition in ^{96}Ru. In a first calculation $B(E\mathcal{L})$ is calculated using $\lambda = 1.1965$ (adjusted to the binding energy of the ground state). This

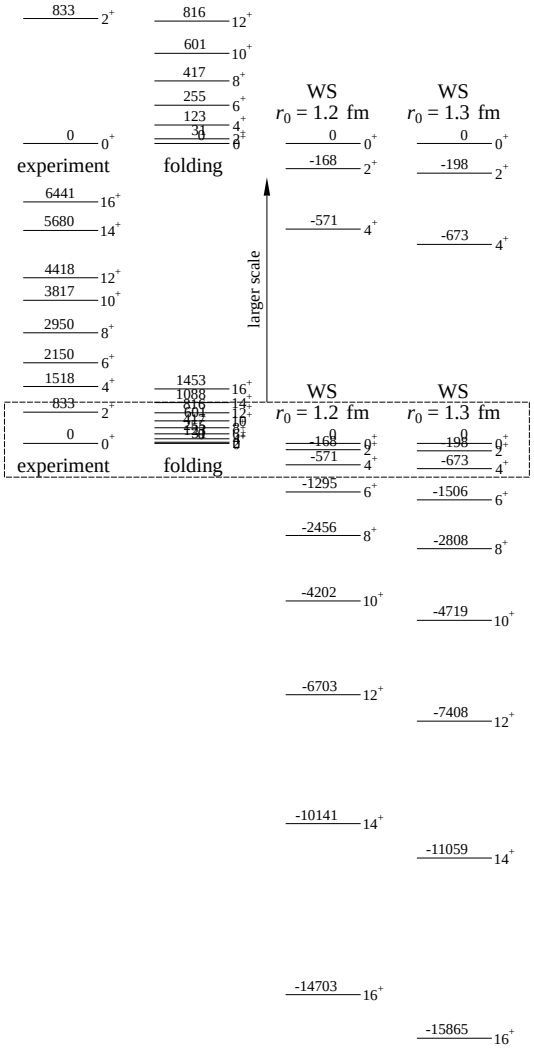

FIG. 2: Excitation energies for the nucleus ^{96}Ru = ^{92}Mo $\otimes$ α. Experimentally one finds a rotational band 0^+, 2^+, 4^+, ... 16^+ (left). Although compressed in energy, the folding potential reproduces such a rotational band (with the energies E_x = 31, 123, 255, 417, 601, 816, 1088, and 1453 keV for the 2^+, 4^+, ... 16^+ states). In contrast, the Woods-Saxon potentials show an inversion of the levels (right). All energies are given in keV. The low-enery region (as indicated by the dashed box) is scaled up in the upper part of the diagram for better readability.

leads to $E_x(2^+) = 31$ keV (as shown in Fig. 2) instead of the experimental $E_x = 833$ keV. In a second calculation the wave function of the 2^+ state is calculated using a slightly changed potential strength $\lambda = 1.1852$ (adjusted to fit the excitation energy of the 2^+ state). The resulting $B(E\mathcal{L})$ value changes only by about 2 % between these two calculations which can be explained by Figs. 1 and 3. The dominating contribution of the integral in Eq. (3) comes from the nuclear interior and surface. However, a change in the excitation energy mainly leads to a change in the asymptotic behavior of the wave function, i.e. a different slope of the wave function in the exterior region.

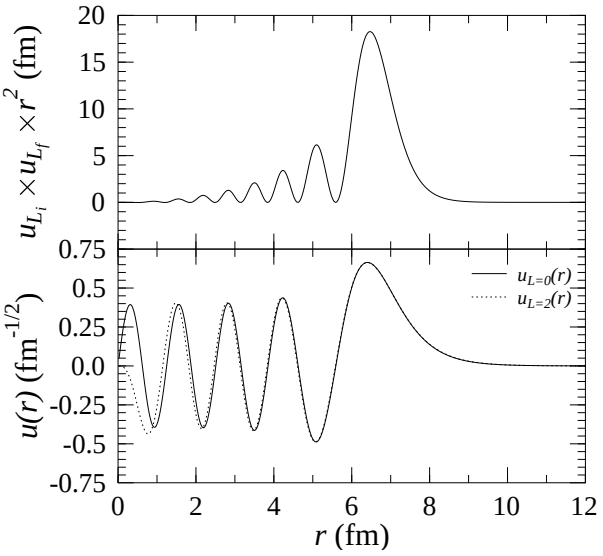

FIG. 3: Wave functions $u_{L=0}(r)$ and $u_{L=2}(r)$ (lower part), and the integrand of the overlap integral in Eq. (3) (upper part) for the transition from the 2^+ state at $E_x = 833$ keV to the 0^+ ground state in ^{96}Ru.

Although the dependence of the $B(E\mathcal{L})$ values on the excitation energy is relatively small, all $B(E\mathcal{L})$ values are calculated from wave functions with correct asymptotic bahavior, i.e. the potential strength has been readjusted to fit the respective excitation energy E_x, see Sect. III and Fig. 5.

III. RESULTS

It is one aim of the present investigation to study the behavior of the potential strength parameter λ of the folding potential for a broad range of $N = 50$ nuclei. As will be shown, the parameter λ shows a very systematic and regular behavior. This can be used to predict up-to-now unknown properties like e.g. α-decay energies or excitation energies [36]. Alternatively, clear deviations from the systematic behavior of the potential strength parameter λ may be interpreted as indications for shell closures [25].

The variation of the potential strength parameter λ and the resulting volume integral J_R are shown in Fig. 4 for $N = 50$ nuclei from ^{78}Ni up to ^{100}Sn. The strength parameter λ has been adjusted to reproduce the binding energies of the nuclei from ^{82}Zn = ^{78}Ni $\otimes$ α to ^{104}Te = ^{100}Sn $\otimes$ α which are taken from [1, 48]. It is obvious from Fig. 4 that both diagrams look very similar. Thus, in the following presentation of the results only the systematics of the strength parameter λ is discussed. A similar systematics is obtained for the volume integrals J_R. Note that minor differences for the potential strength parameter λ for ^{94}Mo = ^{90}Zr $\otimes$ α between this study and earlier work in [4, 12] are the consequence of

the global parametrization for the nuclear density used in this study.

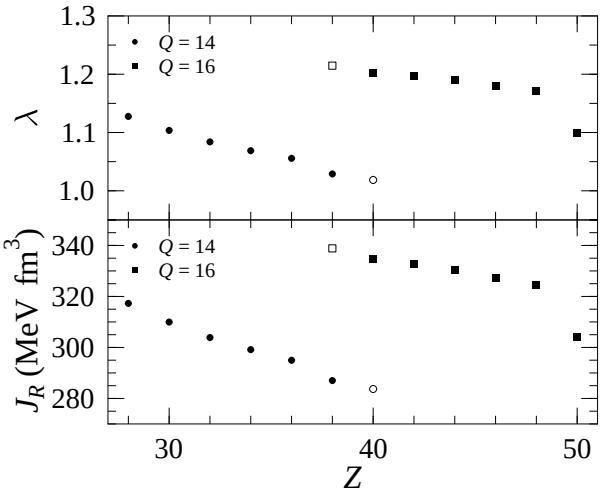

FIG. 4: Potential strength parameter λ (upper part) and volume integrals J_R (lower part) for nuclei (A+4,N=52) = (A,N=50) $\otimes$ α in dependence of the proton number Z. Data for $Z = 50$ are taken from the extrapolation in [36]. Further discussion see text.

The variation of λ in dependence of the proton number Z in Fig. 4 is very smooth except around $Z = 40$ and $Z = 50$. Both discontinuities are related to shell closures. Changes of the volume integral J_R by more than about 10 MeV fm^3 (corresponding to changes in λ by more than about 0.035) are typical for the crossing of a shell closure [25]. Usually, the crossing of a shell closure should be combined with a change of the oscillator quanta Q. However, the situation around the magic number $Z = N = 50$ is complicated by the fact that the $g_{9/2}$ subshell ($q = 4$) is located at relatively low energies close to the p and f subshells with $q = 3$.

From $Z = 48$ to $Z = 50$ the oscillator quanta Q in the model do not change. However, the strength parameter λ changes by about 0.07 which reflects the strong $Z = 50$ shell closure at ^{100}Sn. (The potential parameters for ^{100}Sn have been derived from the systematics of various tin isotopes [36].) Such changes in the potential strength parameter λ may be used to assign unknown magic numbers, e.g. for superheavy nuclei [25].

The discontinuity at the subshell closure at $Z = 40$ between the f and p subshells and the proton $g_{9/2}$ subshell turns out to be an artefact. Below $Z = 40$, the wave functions have been calculated with $Q = 14$, i.e. seven nodes for the $L = 0$ ground state wave function. Above $Z = 40$, the node number has been increased by one to eight nodes ($Q = 16$). Obviously, the potential strength has to be increased significantly to obtain a wave function with an additional node at similar energies. As will be shown in the next paragraph, the change in the potential strength parameter λ is a pure consequence of the changing oscillator quantum number Q of the model.

A simple estimate of the strength of the subshell closure at $Z = 40$ can be obtained as follows. If there is a strong shell closure, a discontinuity in λ should also be observed when passing the shell closure without changing the node number (as in the case around $Z = 50$ discussed above). For this purpose the open symbols in Fig. 4 have been calculated at $Z = 38$ (^{92}Zr = ^{88}Sr $\otimes$ α) with $Q = 16$ (instead of $Q = 14$) and at $Z = 40$ (^{94}Mo = ^{90}Zr $\otimes$ α) with $Q = 14$ (instead of $Q = 16$). From the comparison with neighboring nuclei it is evident that there is no strong shell closure at $Z = 40$ because the variation of λ is very smooth. The physical properties of α-cluster states are thus not affected by the subshell closure at $Z = 40$.

For the example of ^{96}Ru = ^{92}Mo $\otimes$ α it has already been shown in Fig. 2 that the folding potential is able to generate a rotational band. But the calculated excitation energies are lower than the experimental energies. A small readjustment of the potential strength parameter λ for each state of the ground state rotational band is required to obtain the correct excitation energies. This readjustment procedure has been done for all nuclei under study. The result is shown in Fig. 5.

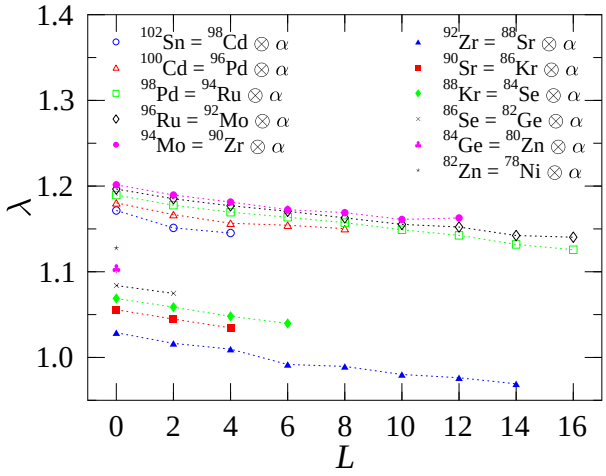

FIG. 5: Potential strength parameter λ as a function of angular momentum L for the ground state rotational bands in (N=50) $\otimes$ α nuclei. For all nuclei λ is slightly decreasing with increasing L.

For all nuclei under study the same behavior is found. The potential strength has to be reduced by less than 1 % for neighboring levels of the rotational band (e.g., between 0^+ and 2^+ states or between 6^+ and 8^+ states). The total change of the strength parameter λ within a rotational band, i.e. the change between the 0^+ ground state and the 14^+ or 16^+ state is about 5 % in all nuclei under study.

It has been suggested in [4, 12] to parametrize the variation in the potential strength parameter λ by

$$\lambda(L) = \lambda(L = 0) - c \times L \qquad (4)$$

where the $\lambda(L = 0)$ values are the required strength

parameters for the ground state binding energies (see Fig. 4). As already pointed out above, the variations in λ are very small. Thus the parameter c is extremely small, and variations in c are hardly visible in Fig. 5. Therefore in Fig. 6 the parameter c is shown separately; it is extracted from all data in Fig. 5. The potential variation parameter c is almost constant for all nuclei and all angular momenta. There is a weak tendency of smaller c values for states with higher angular momenta at higher excitation energies.

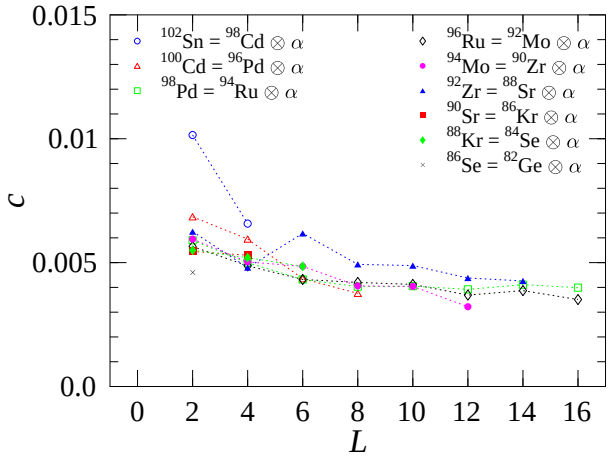

FIG. 6: Variation of the potential strength parameter λ according to Eq. (4): the parameter c is extracted from the previous Fig. 5. By definition, $c = 0$ for $L = 0$ (not shown).

For the first excited 2^+ state the parameter $c(L = 2)$ takes values between about 0.005 and 0.007. This result is illustrated in Fig. 7 where $c(L = 2)$ is plotted against the proton number Z. An average value of $c(L = 2) = 0.0057 \pm 0.0007$ is found for the nuclei between $Z = 32$ and $Z = 46$. An exceptionally large value of $c = 0.0102$ is found for $Z = 48$, i.e., for the first 2^+ state in ^{102}Sn = ^{98}Cd ⊗ α. Again, such an exceptional behavior is a signature of a shell closure. The first excited state of the semi-magic $Z_C = 50$ nucleus ^{102}Sn is located at a relatively high excitation energy of $E_x = 1472\,\mathrm{keV}$ [1]. As a consequence, a relatively small potential strength parameter λ and a relatively strong variation parameter $c(L = 2)$ are required for the correct description of the excitation energy of this 2^+ state. Interestingly, the excitation energy of the 4^+ state in ^{102}Sn can be calculated using a much smaller and almost regular value for $c(L = 4) = 0.0066$ (see Fig. 6).

Experimental data for transition strengths are available for nuclei close to stability whereas almost no transition strengths have been measured for nuclei far from the valley of stability. In Table I the experimentally available transition strength data [1] are compared to the calculated values in the α-cluster model. Additionally, $B(E2)$ values for $2^+ \rightarrow 0^+$ transitions from the first excited 2^+ state to the 0^+ ground state are listed for all nuclei under study. The results in Table I have been calculated without effective charge. In general, the theoretical results deviate by less than a factor of two from the experimental values.

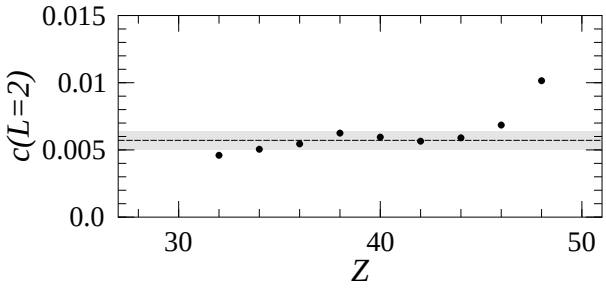

FIG. 7: The parameter $c(L = 2)$ is shown as a function of Z. An average value of $c = 0.0057 \pm 0.0007$ (indicated by the shaded area) is found with the exception of $c = 0.0102$ for $Z = 48$ which results from the $Z_C = 50$ shell closure (see text).

TABLE I: Experimental [1] and calculated transition strengths $B(E\mathcal{L})$ for α-cluster states above $N = 50$ nuclei. All transition strengths are given in Weisskopf units. The result for ^{104}Te has been taken from [36].

nucleus	$L_i \rightarrow L_f$	$B(E2)_{\mathrm{calc}}$	$B(E2)_{\mathrm{exp}}$
^{82}Zn = ^{78}Ni ⊗ α	$2^+ \rightarrow 0^+$	7.1	–
^{84}Ge = ^{80}Zn ⊗ α	$2^+ \rightarrow 0^+$	7.3	–
^{86}Se = ^{82}Ge ⊗ α	$2^+ \rightarrow 0^+$	7.4	–
^{88}Kr = ^{84}Se ⊗ α	$2^+ \rightarrow 0^+$	7.4	–
^{90}Sr = ^{86}Kr ⊗ α	$2^+ \rightarrow 0^+$	7.4	8.4(24)
	$4^+ \rightarrow 2^+$	10.2	5.1(9)
^{92}Zr = ^{88}Sr ⊗ α	$2^+ \rightarrow 0^+$	7.8	6.4(6)
	$4^+ \rightarrow 2^+$	10.6	4.04(12)
	$8^+ \rightarrow 6^+$	9.1	3.59(22)
^{94}Mo = ^{90}Zr ⊗ α	$2^+ \rightarrow 0^+$	8.9	16.0(4)
	$4^+ \rightarrow 2^+$	12.4	26(4)
^{96}Ru = ^{92}Mo ⊗ α	$2^+ \rightarrow 0^+$	8.7	18.0(6)
	$4^+ \rightarrow 2^+$	12.1	21(3)
	$6^+ \rightarrow 4^+$	12.1	12(8)
^{98}Pd = ^{94}Ru ⊗ α	$2^+ \rightarrow 0^+$	8.6	–
^{100}Cd = ^{96}Pd ⊗ α	$2^+ \rightarrow 0^+$	8.5	–
	$8^+ \rightarrow 6^+$	10.5	0.0166(11)
^{102}Sn = ^{98}Cd ⊗ α	$2^+ \rightarrow 0^+$	8.5	–
^{104}Te = ^{100}Sn ⊗ α	$2^+ \rightarrow 0^+$	10.1	–

IV. DISCUSSION

A very smooth variation of the potential strength parameter λ and the variation parameter c has been found for all nuclei under study (see Figs. 4 – 7). This smooth behavior can be used to predict up-to-now unknown properties. As an example, I calculate the excitation energies of the first excited 2^+ states of ^{82}Zn = ^{78}Ni ⊗ α and ^{84}Ge = ^{80}Zn ⊗ α. Properties of ^{104}Te = ^{100}Sn ⊗ α have already been calculated in [36].

From the average value of $c = 0.0057$ for the $L = 2$ states one finds $\lambda(L = 2) = 1.0922$ for the first 2^+ state in ^{84}Ge. The corresponding energy is $E_x = 877\,\mathrm{keV}$. The uncertainty of the potential variation parameter $c(L = 2)$ translates to an uncertainty of about 100 keV for the excitation energy of the 2^+ state in ^{84}Ge. A similar calculation for the first 2^+ state in ^{82}Zn leads to an excitation energy of $E_x = 880\,\mathrm{keV}$, again with an uncertainty of abot 100 keV.

The excitation energy of the first excited 2^+ state in ^{104}Te was estimated in [36] as $E_x \approx 650\,\mathrm{keV}$ using values of $c \approx 0.003 - 0.005$ from very few neighboring nuclei below and above $^{104}\mathrm{Te} = {}^{100}\mathrm{Sn} \otimes \alpha$. Using $c = 0.0057$ from this study of lighter $N = 50$ nuclei, the revised excitation energy is slightly higher: $E_x = 807\,\mathrm{keV}$.

Besides the ground state band, odd-parity and higher-nodal bands have been identified in lighter nuclei, e.g. $^{20}\mathrm{Ne} = {}^{16}\mathrm{O} \otimes \alpha$ and $^{44}\mathrm{Ti} = {}^{40}\mathrm{Ca} \otimes \alpha$ (as reviewed in [4]). The most successful experimental method has been α-transfer in the (^{6}Li,d) reaction [5]. Unfortunately, no experimental (^{6}Li,d) data can be found for the nuclei under study in [1]. Such experiments are difficult because of the relatively high Coulomb barrier for intermediate mass nuclei which leads to small reaction cross sections and because of the increasing level density. Furthermore, experimental studies using the (^{6}Li,d) reaction are almost impossible for unstable $N = 50$ nuclei. Higher-nodal bands have also not been identified in an α-transfer experiment using the ^{90}Zr(^{16}O,^{12}Cγ)^{94}Mo reaction [49].

As an example for higher-nodal bands, I calculate the excitation energies of the band heads of the $Q = 17$ and $Q = 18$ bands in $^{96}\mathrm{Ru} = {}^{92}\mathrm{Mo} \otimes \alpha$ and $^{94}\mathrm{Mo} = {}^{90}\mathrm{Zr} \otimes \alpha$. Using Eq. (4), one finds $E_x \approx 7\,\mathrm{MeV}$ for the 1^-, $Q = 17$ band heads and $E_x \approx 11\,\mathrm{MeV}$ for the 0^+, $Q = 18$ band heads in both nuclei. This finding is in reasonable agreement with earlier estimates for ^{94}Mo [4, 12, 50].

In principle, the calculation of transition strengths from Eq. (3) is straightforward. However, as can be seen from Fig. 3, the integrand in Eq. (3) consists of the product of two oscillating wave functions. Thus, the integrand also oscillates, and the integral depends sensitively on the zeroes of the wave functions, i.e. the radial location of the nodes. This is particularly the case for wave functions with few nodes where positive and negative regions of the integrand in Eq. (3) may cancel each other. For $E2$, $2^+ \rightarrow 0^+$ transitions the dominating contribution comes from the nuclear surface (see Fig. 3), and the calculated $B(E2)$ value is not extremely sensitive to the nodes of the wave functions and does not depend very sensitively on the underlying potential.

In general, the calculated $B(E2)$ values do not deviate by more than a factor of two from the experimental values (see Table I). This must be considered as a quite satisfactory result because the nuclear structure of $A \approx 80 - 100$ nuclei is much more complex than the simple α-cluster description. On the other hand, the reasonable agreement between calculated and experimental $B(E2)$ values confirms that α-clustering is still an important feature for intermediate mass nuclei which has already been pointed out earlier (e.g. [4, 12, 13]).

There is one striking deviation between calculated and experimental $B(E2)$ values in Table I: the strength of the $E2$ transition from the 8^+ isomer at $E_x = 2548\,\mathrm{keV}$ to the 6^+ state at $E_x = 2095\,\mathrm{keV}$ in ^{100}Cd is overestimated by a factor of more than 500. It is a very special feature of the ^{100}Cd nucleus that two 4^+ levels, two 6^+ levels, and two 8^+ levels are located very close to each other: $E_x(4^+) = 1799\,\mathrm{keV}$ and 2046 keV, $E_x(6^+) = 2095\,\mathrm{keV}$ and 2458 keV, $E_x(8^+) = 2548\,\mathrm{keV}$ and 3200 keV [1]. The assignment of each lower state to the ground state band in [1] seems to be at least questionable because of the extremely low transition strength from the 8^+ isomer to the 6^+ state at $E_x = 2095\,\mathrm{keV}$. A larger strength of $B(E2) = 1.8(8)\,\mathrm{W.u.}$ has been found for the transition from the 8^+ isomer to the 6^+ state at $E_x = 2458\,\mathrm{keV}$. Unfortunately, no transition strength is known for the decay of the second 8^+ state at $E_x = 3200\,\mathrm{keV}$ which decays only to the lower 6^+ state at $E_x = 2095\,\mathrm{keV}$. Summarizing the above, a clear band assignment is not possible for ^{100}Cd. Also mixing may occur between states with the same quantum number J^π. Further evidence for inconsistencies in the band assignment and/or mixing can be read from Fig. 6. Here one finds relatively large c values for $L = 2$ and $L = 4$; contrary, the c values for $L = 6$ and $L = 8$ are relatively small.

The present study is restricted to semi-magic $N = 50$ even-even nuclei. An extension to semi-magic $N = 50$ even-odd nuclei is complicated by the additional spin I of the even-odd $N = 50$ core which couples to the angular momentum L of the α-particle and leads to multiplets of α-cluster states. A first attempt for $^{93}\mathrm{Nb} = {}^{89}\mathrm{Y} \otimes \alpha$ has been made together with a study of the ^{89}Y(α,α)^{89}Y scattering cross section [14]. Here I briefly summarize the results of [14]. ^{89}Y has $I^\pi = 1/2^-$ corresponding to neighboring ^{90}Zr with a proton hole in the $p_{1/2}$ subshell. α-cluster states with $L = 0$, $J^\pi = 1/2^-$ and $L = 2$, $J^\pi = 3/2^-$, $5/2^-$ have been clearly identified in ^{93}Nb. The systematics of the potential parameters strengthens a reassignment of J^π of the state at $E_x = 1500\,\mathrm{keV}$ in ^{93}Nb. Whereas $J^\pi = 7/2$ is found in [1], a recent experiment [51] has found strong evidence for $J^\pi = 9/2^-$ and measured a transition strength of $26.4^{+9.7}_{-6.2}\,\mathrm{W.u.}$ for the transition to the $L = 2$, $J^\pi = 5/2^-$ α-cluster state at $E_x = 810\,\mathrm{keV}$. These experimental data [51] confirm that the state at $E_x = 1500\,\mathrm{keV}$ is the $L = 4$, $J^\pi = 9/2^-$ α-cluster state in $^{93}\mathrm{Nb} = {}^{89}\mathrm{Y} \otimes \alpha$.

The folding potential has been calculated throughout this work using a simplistic scaling of the radius parameter of the density of the core nucleus with $r \sim A^{1/3}$. This global parametrization for the density has been applied successfully in a broad mass range [25, 36]. The obtained results do not depend sensitvely on the chosen radius parameter. For a study of this sensitivity, I have increased the radius parameter of the density of ^{92}Mo strongly by 10 %. Because the other ingredients of the folding procedure, i.e. the α-particle density and the interaction,

remain unaffected, the root-mean-square radius of the potential changes by only about 5 %. Although the absolute values of the potential strength change (standard potential: $\lambda = 1.1965$ and 1.1852 for the 0^+ and 2^+ states in ^{96}Ru; increased radius potential: $\lambda = 1.2296$ and 1.2162), the variation c of the potential strength in Eq. (4) remains very small and changes from 0.0057 to 0.0067 (see also Figs. 6 and 7). The calculated $B(E\mathcal{L})$ value for the $2^+ \rightarrow 0^+$ transition in ^{96}Ru increases by about 20 % using the potential with the larger radius. These relatively small changes of the results indicate that the simplistic scaling of the radius parameter in the density parametrization can be used for extrapolations to unstable nuclei with reasonable accuracy.

V. CONCLUSIONS

The α-cluster model has been applied successfully to intermediate mass nuclei above the $N = 50$ shell closure between $^{82}\mathrm{Zn} = {}^{78}\mathrm{Ni} \otimes \alpha$ and $^{104}\mathrm{Te} = {}^{100}\mathrm{Sn} \otimes \alpha$. The underlying double-folding potentials show a systematic and very smooth variation which has been studied in detail. This behavior allows extrapolations with relatively small uncertainties.

The present study is restricted to even-even nuclei. It may be extended to even-odd nuclei although additional complications will arise from the spin of the even-odd $N = 50$ core which leads to multiplets of α-cluster states for each angular momentum $L > 0$.

Transition strengths for $E2$ transitions have been calculated and are in rough agreement with experimental results. A significant deviation for ^{100}Cd may be the result of an inconsistent band assignment in [1] and/or mixing.

The results of the present study confirm that α-clustering is an important feature in intermediate mass nuclei. Experimental data from α transfer reactions, in particular (^{6}Li,d) data, are urgently needed to verify the theoretical predictions and to identify higher-nodal bands in intermediate mass nuclei.

[1] Evaluated and Compiled Nuclear Structure Data ENSDF, *http://www.nndc.bnl.gov/ensdf*.
[2] J. H. Kelley, D. R. Tilley, H. R. Weller, G. M. Hale, Nucl. Phys. **A541**, 1 (1992).
[3] S. Ohkubo, M. Fujiwara, P. E. Hodgson, Prog. Theor. Phys. Suppl. **132**, 1 (1998).
[4] F. Michel, S. Ohkubo, G. Reidemeister, Prog. Theor. Phys. Suppl. **132**, 7 (1998).
[5] T. Yamaya, K. Katori, M. Fujiwara, S. Kato, S. Ohkubo, Prog. Theor. Phys. Suppl. **132**, 73 (1998).
[6] T. Sakuda and S. Ohkubo, Prog. Theor. Phys. Suppl. **132**, 103 (1998).
[7] E. Uegaki, Prog. Theor. Phys. Suppl. **132**, 135 (1998).
[8] M. Hasegawa, Prog. Theor. Phys. Suppl. **132**, 177 (1998).
[9] S. Koh, Prog. Theor. Phys. Suppl. **132**, 197 (1998).
[10] A. Tohsaki, Prog. Theor. Phys. Suppl. **132**, 213 (1998).
[11] P. Mohr, H. Abele, V. Kölle, G. Staudt, H. Oberhummer, H. Krauss, Z. Phys. A **349**, 339 (1994).
[12] S. Ohkubo, Phys. Rev. Lett. **74**, 2176 (1995).
[13] B. Buck, A. C. Merchant, and S. M. Perez, Phys. Rev. C **51**, 559 (1995).
[14] G. G. Kiss, P. Mohr *et al.*, to be published.
[15] U. Atzrott, P. Mohr, H. Abele, C. Hillenmayer, and G. Staudt, Phys. Rev. C **53**, 1336 (1996).
[16] P. Mohr, T. Rauscher, H. Oberhummer, Z. Máté, Zs. Fülöp, E. Somorjai, M. Jaeger, and G. Staudt, Phys. Rev. C **55**, 1523 (1997).
[17] Zs. Fülöp, Gy. Gyürky, Z. Máté, E. Somorjai, L. Zolnai, D. Galaviz, M. Babilon, P. Mohr, A. Zilges, T. Rauscher, H. Oberhummer, and G. Staudt, Phys. Rev. C **64**, 065805 (2001).
[18] D. Galaviz, Zs. Fülöp, Gy. Gyürky, Z. Máté, P. Mohr, T. Rauscher, E. Somorjai, and A. Zilges, Phys. Rev. C **71**, 065802 (2005).
[19] G. G. Kiss, Gy. Gyürky, Zs. Fülöp, Z. Máté, E. Somorjai, D. Galaviz, A. Kretschmer, K. Sonnabend, A. Zilges, Europ. Phys. J. A **27**, s01, 197 (2006).
[20] G. G. Kiss, Gy. Gyürky, Zs. Fülöp, E. Somorjai, D. Galaviz, A. Kretschmer, K. Sonnabend, A. Zilges, P. Mohr, M. Avrigeanu, J. Phys. G, in press.
[21] P. Demetriou, C. Grama, and S. Goriely, Nucl. Phys. **A707**, 253 (2002).
[22] Gy. Gyürky, G. G. Kiss, Z. Elekes, Zs. Fülöp, E. Somorjai, A. Palumbo, J. Görres, H. Y. Lee, W. Rapp, M. Wiescher, N. Özkan, R. T. Güray, G. Efe, T. Rauscher, Phys. Rev. C **74**, 025805 (2006).
[23] E. Somorjai, Zs. Fülöp, A. Z. Kiss, C. E. Rolfs, H.-P. Trautvetter, U. Greife, M. Junker, S. Goriely, M. Arnould, M. Rayet, T. Rauscher, H. Oberhummer, Astron. Astroph. **333** (1998) 1112.
[24] A. Spyrou, H.-W. Becker, A. Lagoyannis, S. Harissopulos, C. Rolfs, Phys. Rev. C **76**, 015802 (2007).
[25] P. Mohr, Phys. Rev. C **73**, 031301(R) (2006); Err.: Phys. Rev. C **74**, 069902(E) (2006).
[26] H. F. Zhang and G. Royer, Phys. Rev. C **76**, 047304 (2007).
[27] C. Samantha and P. R. Chowdhury, Nucl. Phys. **789**, 142 (2007).
[28] C. Xu and Z. Ren, Phys. Rev. C **76**, 027303 (2007).
[29] C. Xu and Z. Ren, Nucl. Phys. A **753**, 174 (2005).
[30] P.-R. Chowdhury, C. Samanta, and D. N. Basu, Phys. Rev. C **73**, 014612 (2006).
[31] V. Yu. Denisov and H. Ikezoe, Phys. Rev. C **72**, 064613 (2005).
[32] P. Mohr, Phys. Rev. C **61**, 045802 (2000).
[33] M. Fujiwara, T. Kawabata, and P. Mohr, J. Phys. G **28**, 643 (2002).
[34] C. Xu and Z. Ren, Nucl. Phys. **A760**, 303 (2005).
[35] C. Xu and Z. Ren, Phys. Rev. C **74**, 037302 (2006).
[36] P. Mohr, Europ. Phys. J. A **31**, 23 (2007).
[37] M. Avrigeanu and V. Avrigeanu, Phys. Rev. C **73**, 038801 (2006).

[38] M. Avrigeanu, W. von Oertzen and V. Avrigeanu, Nucl. Phys. **A764**, 246 (2006).
[39] M. Avrigeanu, W. von Oertzen, A. J. M. Plompen, and V. Avrigeanu, Nucl. Phys. **A723**, 104 (2003).
[40] B. Buck, A. C. Merchant, and S. M. Perez, At. Data Nucl. Data Tab. **54**, 53 (1993).
[41] H. de Vries, C. W. de Jager, and C. de Vries, At. Data Nucl. Data Tables **36**, 495 (1987).
[42] G. R. Satchler and W. G. Love, Phys. Rep. **55**, 183 (1979).
[43] A. M. Kobos, B. A. Brown, R. Lindsay, and R. Satchler, Nucl. Phys. **A425**, 205 (1984).
[44] H. Abele and G. Staudt, Phys. Rev. C **47**, 742 (1993).
[45] F. Hoyler, P. Mohr, and G. Staudt, Phys. Rev. C **50**, 2631 (1994).
[46] B. Buck, A. C. Merchant, S. M. Perez, Phys. Rev. Lett. **72**, 1326 (1994).
[47] B. Buck and A. A. Pilt, Nucl. Phys. **A280**, 133 (1977).
[48] A. H. Wapstra, G. Audi, and C. Thibault, Nucl. Phys. **A729**, 129 (2003).
[49] H. Bohn, G. Daniel, M. R. Maier, P. Kienle, J. G. Cramer, D. Proetel, Phys. Rev. Lett. **29**, 1337 (1972).
[50] F. Michel, G. Reidemeister, S. Ohkubo, Phys. Rev. C **61**, 041601 (2000).
[51] J. N. Orce, C. Fransen, A. Linnemann, C. J. McKay, S. R. Lesher, N. Pietralla, V. Werner, G. Friessner, C. Kohstall, D. Mücher, H. H. Pitz, M. Scheck, C. Scholl, F. Stedile, N. Warr, S. Walter, P. von Brentano, U. Kneissl, M. T. McEllistrem, S. W. Yates, Phys. Rev. C **75**, 014303 (2007).